

# Control of flutter of suspension bridge deck using TMD

Saeid Pourzeynali<sup>†</sup>

*Department of Civil Engineering, Engineering Faculty, Guilan University, Rasht, Iran*

T. K. Datta<sup>‡</sup>

*Department of Civil Engineering, Indian Institute of Technology, Hauz Khas, New Delhi 110 016, India*

**Abstract.** Passive control of the flutter condition of suspension bridges using a combined vertical and torsional tuned mass damper (TMD) system is presented. The proposed TMD system has two degrees of freedom, which are tuned close to the frequencies corresponding to vertical and torsional symmetric modes of the bridge which get coupled during flutter. The bridge-TMD system is analyzed for finding critical wind speed for flutter using a finite element approach. Thomas Suspension Bridge is analyzed as an illustrative example. The effectiveness of the TMD system in increasing the critical flutter speed of the bridge is investigated through a parametric study. The results of the parametric study led to the optimization of some important parameters such as mass ratio, TMD damping ratio, tuning frequency, and number of TMD systems which provide maximum critical flutter wind speed of the suspension bridge.

**Key words:** tuned mass damper; bridge flutter; suspension bridges; passive control.

---

## 1. Introduction

Passive control of structural response due to wind forces has been attempted in the past using various devices. They include tuned mass damper (TMD) (Kihara *et al.* 1993, Weisne 1979), multiple tuned mass damper (MTMD) (Abe and Fujino 1994, Jangid and Datta 1997), active tuned mass damper (ATMD) (Ankireddi and Yang 1996), tuned liquid damper (TLD) (Fujino *et al.* 1992, Sun *et al.* 1991, Yoneda *et al.* 1989), tuned liquid column damper (TLCD) (Xue *et al.* 2000, Sakai *et al.* 1991, Xu *et al.* 1992) and multiple tuned liquid dampers (MTLDs) (Fujino and Sun 1993). Most of these works are reported for buildings. Relatively less work is available on the control of bridge responses. However in recent years, a number of studies on the control of the response of cable-supported bridges under wind-induced forces have been reported. Lin *et al.* (2000) proposed a tuned mass damper, which simultaneously reduces the vertical and torsional buffeting responses of the bridge deck and increases the critical flutter speed of cable-stayed bridges. The proposed system has two frequencies, which are tuned to the frequencies of the first flexural and torsional structural modes, to suppress the resonant effects. Wilde and Fujino (1998) applied an active aerodynamic control method of suppressing flutter of a very long-span bridge. This control system consists of additional control surfaces attached to the bridge deck. The torsional movement of proposed surfaces, commanded via

---

<sup>†</sup> Research Scholar

<sup>‡</sup> Professor

feedback control law, is used to generate stabilizing aerodynamic forces. Wilde *et al.* (1998) also presented a passive aerodynamic control of bridge flutter by adding two additional surfaces to generate stabilizing forces and by putting an additional pendulum to control the torsional motion. Experimental study was also conducted and very good agreement between experimental and theoretical predictions was observed. There have been also some studies to control the flutter of long span bridges using eccentric mass on the bridges. The results were encouraging and were thought to be a possible practical method for suppressing the onset of flutter (Branceleoni 1992, Phongkumsing *et al.* 1998, and Wild *et al.* 1996).

The use of TMD for suppressing the coupled flutter of suspension bridge decks has been attempted by several researchers (Dung *et al.* 1996, Gu *et al.* 1999, and Nobuto *et al.* 1988). The Routh-Hurwitz stability criteria was used to study the aerodynamic instability of the bridge. A model test was also carried out to confirm the numerical results of the control problem (Gu *et al.* 1998). Kobayashi and Nagaoka (1992), and Kobayashi *et al.* (1998) attempted active control of flutter of suspension bridges by ailerons. The exerted force to suppress the flutter condition follows a rule base formulation. Miyata *et al.* (1994) also proposed an active control strategy for the coupled flutter problem for long span bridges.

As such, the control of long span flexible bridges for wind and earthquake excitations is extremely important since such bridges can have large vibrations due to these effects. While earthquake-induced large deformation is an infrequent phenomenon, the wind-induced vibration in long-span bridge, like cable-supported bridges can frequently occur. Although in recent years, there have been several studies on the control of coupled flutter of long span suspension bridges as reported above, the subject requires more attention to explore the best practical method of controlling the bridge flutter. Some of the issues regarding the control of flutter by TMD also need more investigation, such as control of stiffness driven coupled flutter, optimum tuning frequency, optimum damping ratio of the TMD, etc.

In this paper, the tuned mass damper (TMD) system is used to control the flutter condition of suspension bridges using the finite element method of analysis. As the flutter instability of suspension bridges is caused by the self-excited aerodynamic forces, which may lead to coupling between torsional and vertical vibration modes, a combined model of vertical and torsional TMD system is used to control the flutter condition. The two degrees of freedom of the TMD system is tuned close to the frequencies of the vertical and torsional modes of the bridge which get coupled during the flutter. The bridge-TMD system is analyzed to obtain the critical flutter speed. As the numerical study, the Thomas suspension bridges are selected. The increase in the critical flutter speed due to the presence of the TMD system is investigated under a set of parametric variations. The parameters include tuning frequencies, mass ratio, TMD damping ratio and number of TMDs. The optimum values of the parameters are obtained for maximum increase in the flutter speed.

## 2. Assumptions

The following assumptions are made in the analysis, similar to those used by Abdel-Ghaffar (1979, 1980):

1. All stresses in the bridge elements obey the Hooke's law, and therefore no material non-linearity is considered.
2. The initial dead load is carried by cables without causing any stress in the suspended structure.
3. The cable is assumed to be of a uniform cross section and of a parabolic profile under dead load such that the weight of the cable can be assumed to be uniformly distributed along the span instead of along the length of the cable.
4. The hangers (or suspenders) are assumed to be vertical and inextensible, and their forces are

considered to be distributed loads as if the distance between the suspenders were very small.

5. The original shape of every cross-section of the bridge deck is unaltered during vibration although the section may undergo out-of-plane deformation (Warping). Also, the peripheral bending in the walls of the section is negligible.
6. It is assumed that there is no tower resistance to displacement at the tower top and so the horizontal components of the cable tension  $H_w$ , (due to dead load) and  $H(t)$ , (due to dynamic load) are the same on both sides of the tower.

### 3. Equation of motion of the bridge without TMD

In general, there are two approaches that are being used in flutter analysis of suspension bridges: continuum approach and finite element approach. In the present study, the latter approach is used. For this purpose, the entire bridge is discretized into two-dimensional beam elements, each consisting of two nodes at its ends. At each node four degrees of freedom, as shown in Figs. 1(b) and 1(c), are considered.

The governing equation of motion can be written as

$$[\mathbf{M}]\{\ddot{x}\} + [\mathbf{C}]\{\dot{x}\} + [\mathbf{K}]\{x\} = \{F\} \quad (1)$$

where  $[\mathbf{M}]$  is the consistent mass matrix;  $[\mathbf{C}]$  is the structural damping matrix;  $[\mathbf{K}]$  is the structural stiffness matrix;  $\{F\}$  is the  $(4\mathbf{n} \times 1)$  vector of aeroelastic forces; and  $\{x\}$  is the  $(4\mathbf{n} \times 1)$  response vector defined as follows:

$$\{x\} = \{x_1, x_2, \dots, x_{4n}\}_{1 \times 4n}^T \quad (2)$$

in which  $\mathbf{n}$  is the number of nodes along the total bridge length;  $x_i$  is the bridge response at  $i$ th degree of freedom. Note that the aeroelastic forces for bending rotation and warping degrees of freedom (Figs. 1(b) and (c)) are zeroes.

The aeroelastic or self-excited forces acting per unit length of the bridge span as shown in Figs. 2 (a) and (b), may be written as (Jain *et al.* 1996)

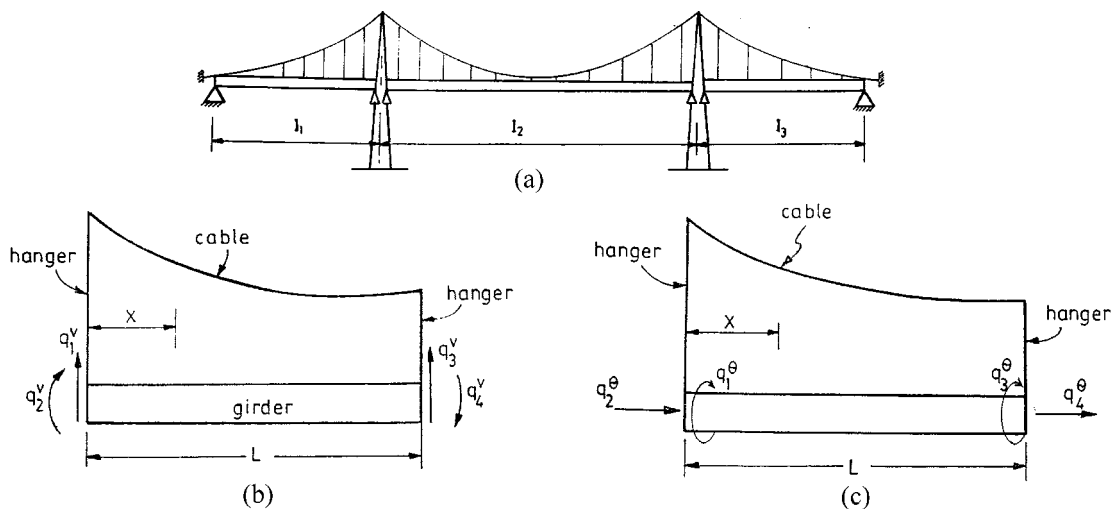


Fig. 1 (a) Suspension bridge model; (b) bridge element with vertical displacement; and (c) bridge element with torsion

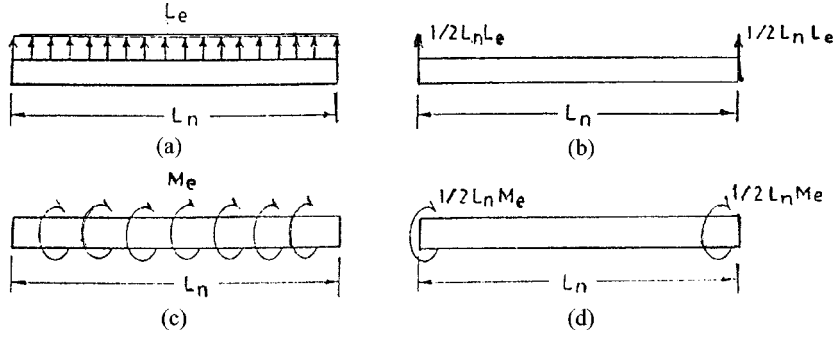


Fig. 2 Self excited forces: (a) distributed vertical load; (b) distributed torsional moment; (c) lumped vertical load; and (d) lumped torsional moment.

$$L_e = \frac{1}{2} \rho U^2 B \left[ k H_1^* \frac{\dot{h}}{U} + k H_2^* \frac{B \dot{\theta}}{U} + k^2 H_3^* \theta + k^2 H_4^* \frac{h}{B} \right] \quad (3a)$$

$$M_e = \frac{1}{2} \rho U^2 B^2 \left[ k A_1^* \frac{\dot{h}}{U} + k A_2^* \frac{B \dot{\theta}}{U} + k^2 A_3^* \theta + k^2 A_4^* \frac{h}{B} \right] \quad (3b)$$

in which  $\rho$  is air mass density;  $U$  is mean wind velocity;  $B$  is bridge deck width;  $k = B\omega/U$  = the reduced frequency;  $\omega$  is the circular response frequency;  $H_i^*$  and  $A_i^*$ ,  $i=1$  to 4 are functions of  $k$  and are the experimentally determined flutter derivatives for the deck cross-section under investigation. Over dots indicate the time derivative. These forces are considered to be constant along the element. In order to evaluate the aeroelastic force vector  $\{F\}$  in Eq. (1), the distributed aeroelastic forces are lumped at the element nodes as shown in Figs. 2 (c) and (d).

The mass and stiffness matrices in Eq. (1) may be expressed as

$$[\mathbf{M}] = \begin{bmatrix} \mathbf{M}^V & / & \text{zeros} \\ \text{---} & / & \text{---} \\ \text{zeros} & / & \mathbf{M}^\theta \end{bmatrix}_{(4n \times 4n)} \quad (4)$$

$$[\mathbf{K}] = \begin{bmatrix} \mathbf{K}^V & / & \text{zeros} \\ \text{---} & / & \text{---} \\ \text{zeros} & / & \mathbf{K}^\theta \end{bmatrix}_{(4n \times 4n)} \quad (5)$$

where  $\mathbf{M}^V$  and  $\mathbf{K}^V$  are the mass and stiffness matrices, respectively in bending vibration; and  $\mathbf{M}^\theta$  and  $\mathbf{K}^\theta$  are those of the torsional vibration. Using the total potential and kinetic energies of the bridge and applying the Hamilton's principle, the structural mass and stiffness matrices of the system can be evaluated (Abdel-Ghaffar 1979, 1980). The structural damping matrix  $[\mathbf{C}]$  is assumed to be a proportional matrix to both mass and stiffness matrices as

$$[\mathbf{C}] = a_0 [\mathbf{M}] + a_1 [\mathbf{K}] \quad (6)$$

in which  $a_0$  and  $a_1$  are the proportionality constants and are obtained using first two vertical and torsional modes of the bridge (Clough and Penzien 1993).

Using the Eqs. (3), the  $(4n \times 1)$  aeroelastic force vector  $\{F\}$  can be expressed as below :

$$\{F\} = \frac{1}{2}\rho U^2 B \left(\frac{k}{U}\right) [\mathbf{A}^F] \{\dot{x}\} + \frac{1}{2}\rho U^2 B k^2 [\mathbf{B}^F] \{x\} \quad (7)$$

where  $\{x\}$  is defined in Eq. (2); and matrices  $[\mathbf{A}^F]$  and  $[\mathbf{B}^F]$  are given in the Appendix-A. Substituting Eq. (7) into Eq. (1), the final equation of motion can be expressed as

$$[\mathbf{M}]\{\ddot{x}\} + [\mathbf{C}]\{\dot{x}\} + [\mathbf{K}]\{x\} = \frac{1}{2}\rho B^2 \omega [\mathbf{A}^F] \{\dot{x}\} + \frac{1}{2}\rho B^3 \omega [\mathbf{B}^F] \{x\} \quad (8)$$

#### 4. Equation of motion of the bridge with TMD

The TMD system is placed at the  $i$ th node of the bridge span as shown in Fig. 3. The TMD system has both vertical and torsional degrees of freedom. Therefore, the bridge-TMD system has two additional degrees of freedom. When more than one TMD are used, the additional degrees of freedom are  $2r$ , in which  $r$  is the number of TMD systems used. Stiffness and damping parameters of the TMD are determined from the assumed mass of the TMD and the tuning frequencies. Thus, the TMD parameters are given by

$$K_{Ti}^V = M_{Ti}^V (\omega^V)^2 \quad (9)$$

$$K_{Ti}^\theta = I_{Ti}^\theta (\omega^\theta)^2 \quad (10)$$

$$C_{Ti}^V = 2\zeta_{Ti}^V M_{Ti}^V \omega^V \quad (11)$$

$$C_{Ti}^\theta = 2\zeta_{Ti}^\theta I_{Ti}^\theta \omega^\theta \quad (12)$$

where  $\omega^V$  and  $\omega^\theta$  are the vertical and torsional tuning frequencies;  $C_{Ti}^V$  and  $C_{Ti}^\theta$  are the vertical and torsional damping coefficients;  $M_{Ti}^V$  and  $I_{Ti}^\theta$  are the masses of the TMD corresponding to vertical and torsional degrees of freedom;  $\zeta_{Ti}^V$  and  $\zeta_{Ti}^\theta$  are the vertical and torsional damping ratios and  $i$

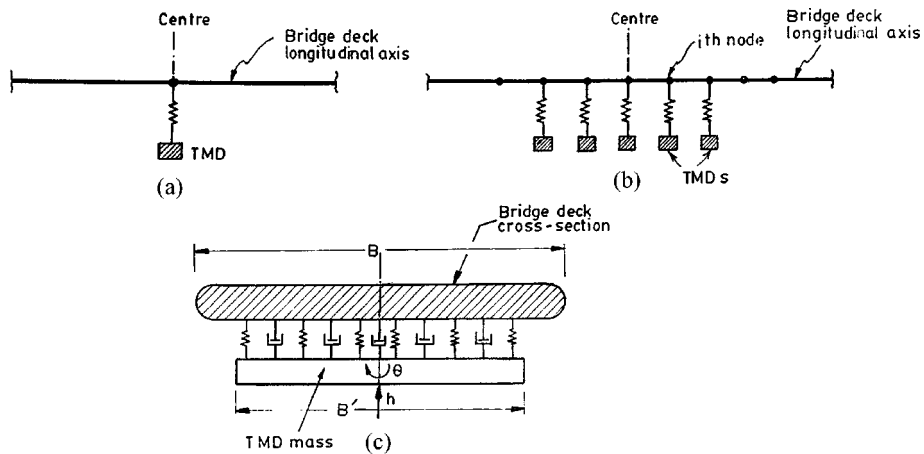


Fig. 3 Bridge and TMD system: (a) longitudinal elevation of deck (single TMD); (b) longitudinal elevation of the deck (multiple TMD); and (c) bridge deck cross section at  $i$ th node.

denotes the number of the node where the TMD is placed. Note that a TMD is spread along the width of the bridge deck as shown in Fig. 3. The mass matrix  $[\mathbf{M}_{BT}]$ , damping matrix  $[\mathbf{C}_{BT}]$  and stiffness matrix  $[\mathbf{K}_{BT}]$  of the combined bridge-TMD are given in the Appendix-A for one TMD placed at the  $i$ th node of the bridge deck. When more than one TMD are used, the corresponding matrices for the bridge-TMD system can be exactly derived by expanding the matrices given in the Appendix-A. The flutter equation of the bridge-TMD system can then be written as

$$[\mathbf{M}_{BT}]\{\ddot{x}_{BT}\} + [\mathbf{C}_{BT}]\{\dot{x}_{BT}\} + [\mathbf{K}_{BT}]\{x_{BT}\} = \frac{1}{2}\rho B^2 \omega [\mathbf{A}_{BT}^F]\{\dot{x}_{BT}\} + \frac{1}{2}\rho B^3 \omega [\mathbf{B}_{BT}^F]\{x_{BT}\} \quad (13)$$

where  $\{x_{BT}\}$  is the  $[(4\mathbf{n}+2r) \times 1]$  structural displacement vector of bridge-TMD system; and  $[\mathbf{A}_{BT}^F]$  and  $[\mathbf{B}_{BT}^F]$  are square matrices of size  $(4\mathbf{n}+2r)$  which are derived from matrices  $[\mathbf{A}^F]$  and  $[\mathbf{B}^F]$  given in the Appendix-A by considering columns and rows corresponding to the TMD system as zeroes. It is noted that the effect of self-excited wind forces on the TMD system is assumed to be negligible.

For applying the multi-mode flutter analysis, the displacement vector  $\{x_{BT}\}$  can be written in terms of (undamped) modal matrix  $[\Phi_{BT}]_{[(4\mathbf{n}+2r) \times \mathbf{m}]}$  of the bridge-TMD system and modal coordinate vector  $\{\xi(t)\}$  as :

$$\{x_{BT}\} = [\Phi_{BT}]\{\xi(t)\}_{\mathbf{m} \times 1} \quad (14)$$

and

$$\{\xi(t)\} = \begin{Bmatrix} \xi_1(t) \\ \xi_2(t) \\ \vdots \\ \xi_{\mathbf{m}}(t) \end{Bmatrix} \quad (15)$$

where  $\mathbf{m}$  is the number of modes considered. Using modal transformation, the flutter equation of the system may be written in modal coordinates as

$$[\bar{\mathbf{M}}_{BT}]\{\ddot{\xi}\} + [\bar{\mathbf{C}}_{BT}]\{\dot{\xi}\} + [\bar{\mathbf{K}}_{BT}]\{\xi\} = \{0\} \quad (16)$$

where

$$[\bar{\mathbf{M}}_{BT}] = [\Phi_{BT}]^T [\mathbf{M}_{BT}] [\Phi_{BT}] \quad (17)$$

$$[\bar{\mathbf{C}}_{BT}] = [\Phi_{BT}]^T [\mathbf{C}_{BT}] [\Phi_{BT}] - \frac{1}{2}\rho B^2 \omega [\mathbf{D}] \quad (18)$$

$$[\bar{\mathbf{K}}_{BT}] = [\Phi_{BT}]^T [\mathbf{K}_{BT}] [\Phi_{BT}] - \frac{1}{2}\rho B^3 \omega^2 [\mathbf{E}] \quad (19)$$

and

$$[\mathbf{D}] = [\Phi_{BT}]^T [\mathbf{A}_{BT}^F] [\Phi_{BT}], \quad [\mathbf{E}] = [\Phi_{BT}]^T [\mathbf{B}_{BT}^F] [\Phi_{BT}] \quad (20)$$

The final flutter equation of the system is solved by putting  $\{\xi\} = \{a\}e^{i\omega t}$ , ( $i = \sqrt{-1}$ ). This leads to

$$[\mathbf{W}]_{\mathbf{m} \times \mathbf{m}} \{a\}_{\mathbf{m} \times 1} = \{0\} \quad (21)$$

in which  $\{a\} = \{a_1, a_2, \dots, a_{\mathbf{m}}\}^T$  is the flutter mode-shape, which indicates the relative participation

of each structural mode in flutter; and the matrix  $[\mathbf{W}]$  is expressed as :

$$[\mathbf{W}] = ([\bar{\mathbf{K}}_{BT}] - \omega^2[\bar{\mathbf{M}}_{BT}]) + i[\bar{\mathbf{C}}_{BT}] \quad (22)$$

Eq. (21) is the well-known eigen-value problem, and its solution provides the flutter condition for the bridge-TMD system. Since the matrix  $[\mathbf{W}]$  is a complex matrix, the condition  $\det[\mathbf{W}]=0$ , requires that both the real and imaginary parts of the determinant be simultaneously zero. This is achieved by the method of trial, in which the value of the reduced frequency,  $k$  is systematically changed until both parts of the determinant are zero at the same  $\omega$ . The critical flutter speed can be evaluated as

$$U_f = \frac{B\omega_f}{k_f} \quad (23)$$

where  $k_f$  and  $\omega_f$  are the values of  $k$  and  $\omega$  respectively for which Eq. (21) is satisfied.

## 5. Numerical example

As a numerical example, the Vincent-Thomas Suspension Bridge located between San Pedro and Terminal Island in Los Angeles County, California is chosen. For this three-span suspension bridge, the structural data are taken from the literature, Abdel-Ghaffar (1979).

The stiffening girder is assumed to be hinged at the ends in each span, and the cables are free to move at the tower top (i.e., roller type cable connection). The number of elements in the side spans,  $N_1=N_3$ , was taken to be 11 elements, and those for the center span,  $N_2$  was taken as 28 elements.

The approximate theoretical expressions for the flutter derivatives for the bridge deck may be written as (Scanlan and Tomko 1971)

$$\begin{aligned} A_1^* &\approx 0; & H_1^* &= -0.8y && \text{for all } y \\ A_2^* &= -0.1436 \sin(0.5984y) && 0 \leq y \leq 5.25 \\ A_2^* &= 0.08422y - 0.4411 && 5.25 < y \\ H_2^* &= 0 && 0 \leq y \leq 5 \\ H_2^* &= 0.00582y^3 - 0.0121y^2 - 0.60252 && 5 < y \\ A_3^* &= 0 && 0 \leq y \leq 2 \\ A_3^* &= 0.2y - 0.4 && 2 \leq y \leq 6 \\ A_3^* &= 0.3y - 1 && 6 < y \\ H_3^* &= 0 && 0 \leq y \leq 4 \\ H_3^* &= -0.011666y^3 + 0.11y^2 - 1.41334y + 4.64003 && 4 < y \end{aligned} \quad (24)$$

in which  $y = \frac{2\pi}{k}$ ;  $k = \frac{B\omega}{U}$ .

Since the values of  $H_4^*$  and  $A_4^*$  for this bridge are not available, they are assumed to be negligible. The given approximate theoretical values of flutter derivatives are plotted in Fig. 4. The

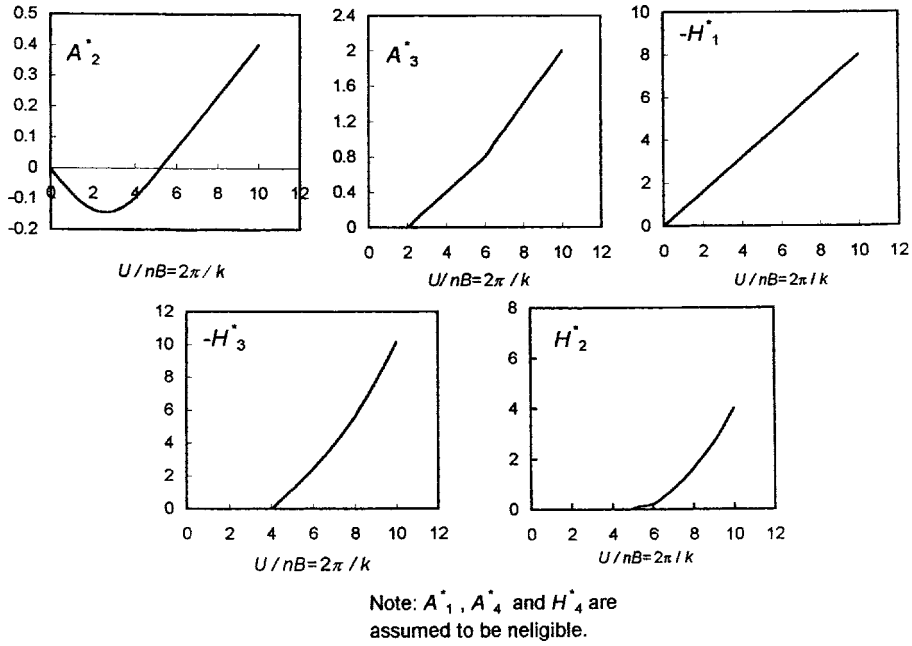


Fig. 4 Approximate flutter derivatives Eq. (24) of Thomas Suspension Bridge

TMD properties are taken as

$$M_{Ti}^V = 7\% \text{ of total bridge mass} = 5.8 \times 10^5 \text{ kg};$$

$$K_{Ti}^V = (1.3743)^2 M_{Ti}^V = 1095446.3 \text{ N/m};$$

(tuned to 1<sup>st</sup> symmetric frequency of the bridge)

$$I_{Ti}^\theta = M_{Ti}^V r^2 = 5.8 \times 10^2 \times 5^2 = 1.45 \times 10^7 \text{ kg-m}^2;$$

$$K_{Ti}^\theta = (3.1163)^2 I_{Ti}^\theta = 1.41 \times 10^8 \text{ N-m};$$

(tuned to 1<sup>st</sup> symmetric torsional frequency)

$$\zeta_{Ti}^V = \zeta_{Ti}^\theta = 2\%$$

The numerical results are obtained with the values of above parameters unless mentioned otherwise.

### 5.1. Free vibration

The results of the free vibrational analysis (first 19 frequencies and first 6 mode shapes) are respectively shown in Table 1 and Fig. 5. In the figure,  $V$  and  $T$  refer to vertical and torsional respectively, and  $A$  and  $S$  refer to anti-symmetric and symmetric, respectively. It is seen that the first five modes correspond to the vertical mode of vibration. Note that free vibrational mode shapes are either purely vertical or purely torsional as it would be expected.



Table 1 Modal properties of Vincent-Thomas Suspension Bridge

Mode No.	Frequency $\omega$ ( rad /sec.)	Mode type	Modal mass ( $\bar{m}$ )
1	1.2324	V-AS	2459813.72
2	1.3743	V-S	2241151.36
3	2.1595	V-AS	1691846.37
4	2.1744	V-S	2835117.10
5	2.8710	V-S	2473230.58
6	3.1163	T-S	97988365.63
7	3.4215	V-AS	2587940.03
8	4.4124	T-AS	104389535.3
9	5.0012	V-S	2370506.36
10	6.68024	T-AS	71798615.43
11	6.7388	T-S	127314525.1
12	6.8351	V-AS	853012.18
13	6.8352	V-S	1021244.00
14	6.8791	V-AS	2460065.24
15	7.0556	T-S	90569439.11
16	9.1062	V-S	2441548.53
17	9.2418	T-AS	1098227534.8
18	11.6557	V-AS	2587889.91
19	11.9381	T-S	103285020.90

Note: T=torsional; V=vertical; S=symmetric; AS=anti-symmetric

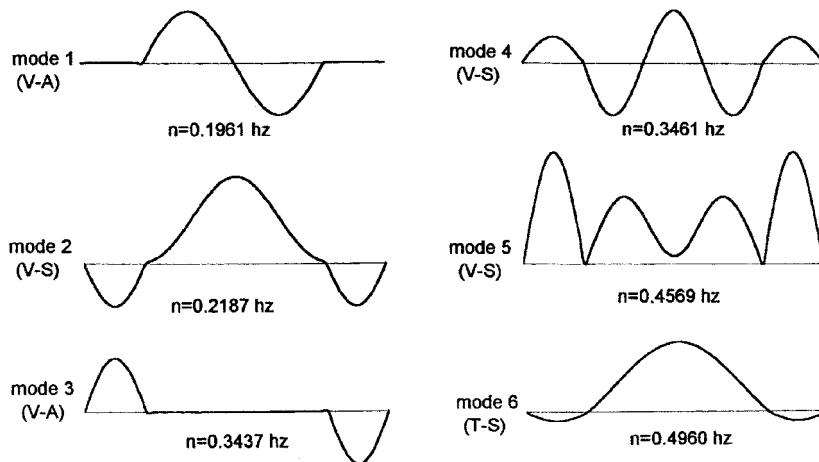


Fig. 5 First six free vertical and torsional vibration mode-shapes

## 5.2. Flutter

Table 2 shows the relative participation of different modes in the flutter for three cases namely, (i) 6-mode analysis; (ii) 7-mode analysis and (iii) 10-mode analysis for the bridge without TMD. It is seen from the table that the 6th mode (i.e., the first symmetric torsional mode) is the predominant mode for the flutter condition. This mode gets coupled with the 2nd and 5th modes, which are the first and third vertical symmetric modes, respectively for the flutter condition. The contributions of the other modes in flutter occurrence are very less in comparison with these modes. Thus, consideration of first

Table 2 Relative flutter mode participation

Case	Magnitude : $ a_i $									
	Mode No.									
	1	2	3	4	5	6	7	8	9	10
	$\times 10^{-7}$	$\times 10^{-2}$	$\times 10^{-18}$	$\times 10^{-4}$	$\times 10^{-1}$	$\times 1$	$\times 10^{-10}$	$\times 10^{-7}$	$\times 10^{-4}$	$\times 10^{-9}$
1	7.8630	8.2849	1.2820	7.0984	1.7827	1.0	—	—	—	—
2	8.7197	9.1670	3.0392	7.8965	1.9034	1.0	4.2003	—	—	—
3	7.8998	9.1670	1.7308	7.8965	1.9034	1.0	4.0899	9.1579	6.5869	2.2922

six modes for the flutter analysis is sufficient. The same observation is made for the bridge-TMD system. Therefore, for further parametric studies first six modes are considered in the analysis. The flutter speed for the bridge alone, for a damping ratio of 0.6%, is  $U_f = 51.8$  m/sec. For a single TMD (Fig. 3(a)) placed at the center, the flutter speed is obtained as  $U_f = 63.02$  m/sec (for TMD mass ratio of 7%), which shows a 21.7% increase in the flutter speed. The effectiveness of TMD in increasing the flutter speed is investigated by conducting a parametric study. The parameters include the TMD mass and damping ratios, tuning frequencies and the number of TMDs.

### 5.3. Effect of mass ratio on the flutter speed

The effect of the ratio of the TMD mass to total bridge mass (mass ratio) on the flutter speed is shown in Fig. 6. The effect is shown for a TMD damping ratio of 3% for both vertical and torsional degrees of freedom. It is seen from the figure that the flutter speed increases with the increase in the mass ratio up to a certain value and then, it remains almost insensitive to the variation of the mass ratio. There is practically no change in the flutter speed beyond a mass ratio of 7%. For this mass ratio, the increase in the flutter speed is about 30%. This shows that there exists an optimum mass ratio beyond which no significant improvement of the stability against flutter can be achieved with the help of a single TMD. Further, it is seen from the figure that the use of a mass ratio of 3% lowers the flutter speed marginally from that obtained with 7% mass ratio (i.e., 67.33 m/sec to 65.79 m/sec). Therefore, it is more realistic to use 3% mass ratio for the control of the flutter speed using

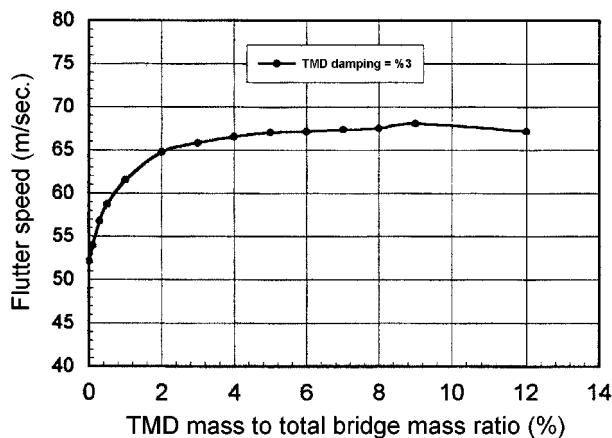


Fig. 6 Effect of mass ratio on the flutter speed

TMD. For further parametric study, 3% mass ratio is used.

#### 5.4. Effect of tuning frequency on the flutter speed

In order to obtain the effect of tuning frequencies on the flutter speed, the vertical and torsional frequencies of the TMD are changed keeping the TMD mass as 3% of the total mass of the bridge. By changing the frequencies, various ratios of vertical frequency of TMD to the third vertical frequency of the bridge ( $r_v$ ) and torsional frequency of the TMD to the first torsional frequency of the bridge ( $r_t$ ) are obtained. Note that the modes corresponding to these bridge frequencies get coupled during flutter. For different pairs of these frequency ratios, the flutter speed for the bridge is obtained for a TMD damping ratio equal to 2% and 5%. The variation of the flutter speed with the pair of frequency ratios is shown in Fig. 7. Pairs of frequency ratios are shown as ( $r_v$ ,  $r_t$ ) in the figure. It is seen from the figure that there exists a pair of frequency ratios for which the flutter speed becomes maximum. The corresponding TMD frequencies are the optimum tuning frequencies. For the example problem, the optimum tuning frequencies are such that the torsional frequency of the TMD is about 0.8 times the first torsional frequency of the bridge, while the vertical frequency of the TMD is about 1.2 times the 3rd vertical frequency of the bridge. Thus, maximum control of the flutter condition is not achieved when TMD frequencies perfectly match with the bridge frequencies. At the optimum tuning frequencies, the flutter speed is about 1.43 times the uncontrolled flutter speed for 2% TMD damping ratio, and is about 2.03 times the uncontrolled flutter speed for 5% TMD damping ratio. Further, it is observed that the effect of the damping of the TMD on the control of flutter is maximum at the optimum tuning frequencies.

#### 5.5. Effect of TMD damping ratio on the flutter speed

Fig. 8 shows the effect of TMD damping ratio on the flutter speed. It can be seen from the figure that the damping of the TMD has significant effect on improving the flutter condition of the bridge. With very small damping of the TMD (i.e., 2% or 5%), it is not possible to obtain much control of the flutter

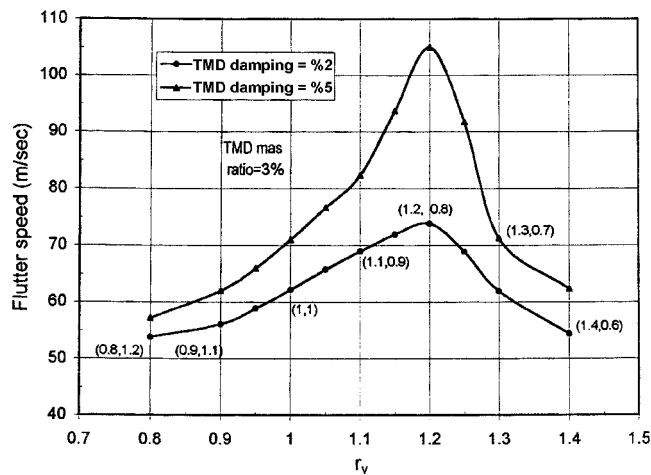


Fig. 7 Effect of tuning frequencies on the flutter speed (TMD mass is 3%)

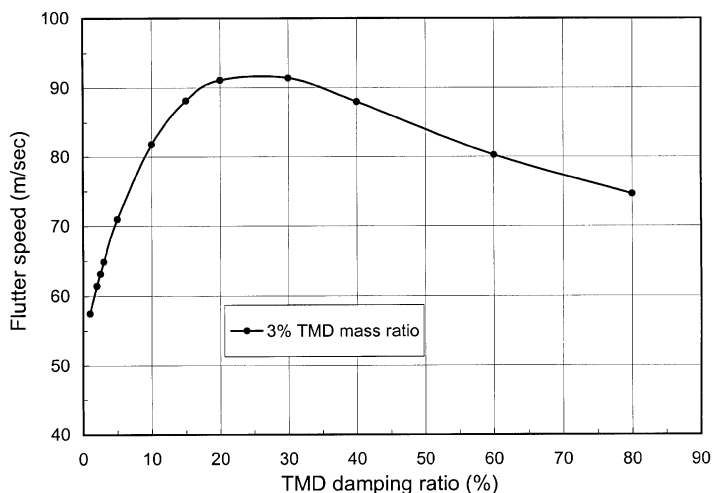


Fig. 8 Effect of TMD damping ratio on the flutter speed (structural damping is 0.6%)

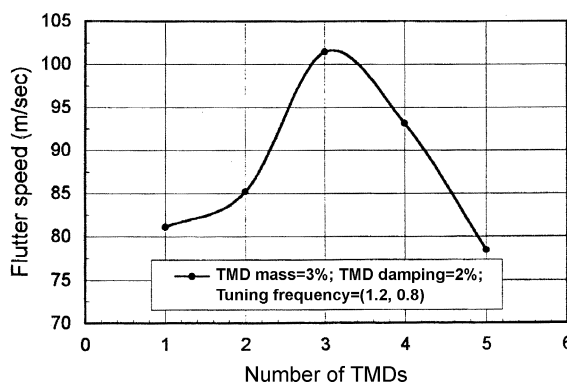


Fig. 9 Effect of the number of TMDs on the flutter speed

condition of the bridge. There will be practically no increase in the flutter speed if only a spring-mass system is suspended from the bridge deck. However, if the damping is increased to about 20%, there is a substantial increase in the flutter speed (1.76 times the uncontrolled flutter speed). Further, it is observed that there is an optimum damping ratio for the TMD for which the maximum control is achieved.

### 5.6. Effect of the number of TMD devices on the flutter speed

In order to study the effect of the number of TMD devices on the flutter speed, a number of TMD devices are arranged symmetrically in the middle of the center span of the bridge as shown in Fig. 3(b). For each TMD, the mass ratio, damping ratio and the tuning frequency ratios are taken as 3%, 2% and (1.2, 0.8) respectively. The variation of flutter wind speed with the number of TMDs is shown in Fig. 9. The variation shows a definite maximum. The maximum flutter speed is obtained for three numbers of TMD devices put in the middle of the center span of the bridge. The corresponding flutter speed is 101.23 m/sec, 1.95 times the uncontrolled flutter speed. Thus, there exists an optimum number of TMD that produces the best control.

## 6. Conclusions

A method of passive control of suspension bridge deck flutter condition using TMD is presented. The proposed passive control technique uses a TMD system, which has coupled vertical-torsional characteristic and therefore, is effective in controlling the aerodynamic coupled flutter of the bridge deck. The effectiveness of the control scheme is investigated through a parametric study. From the results of the parametric study, the following conclusions can be drawn

1. Significant increase in the flutter speed can be achieved by suspending TMDs from the bridge deck. The amount of increase in the flutter speed depends upon the mass ratio, TMD damping ratio, tuning frequencies and the number of TMDs.
2. For practical purposes the optimum mass ratio of the single TMD for the example problem may be taken as 3%.
3. The TMD damping has a significant effect on the flutter speed. There exists an optimum damping ratio for the TMD for which maximum increase in flutter wind speed is achieved.
4. Tuning frequencies have the maximum effect on the flutter speed. Maximum increase in the flutter speed is achieved by tuning TMD frequencies (vertical and torsional) close (but not exactly equal) to the frequencies of the bridge modes which get coupled during flutter. For the example problem, tuning frequencies are 1.2 times and 0.8 times the 3rd vertical and first torsional frequencies of the bridge, respectively.
5. Flutter speed does not monotonically increase with the increase in the number of TMDs suspended from the bridge deck. There is an optimum number of TMDs for which maximum increase in the flutter speed is achieved. For the example problem, this number is three.

## References

- Abdel-Ghaffar, A.M. (1980), "Vertical vibration analysis of suspension bridges", *J. Struct. Div.*, ASCE, **106**(10), 2053-2074.
- Abdel-Ghaffar, A.M. (1979), "Free torsional vibrations of suspension bridges", *J. Struct. Div.*, ASCE, **105**(4), 767-789.
- Abe, M. and Fujino, Y. (1994), "Dynamic characterization of multiple tuned mass dampers and some design formulas", *J. Earthquake Eng. Struct. Dyn.*, **23**(8), 813-835.
- Ankireddi, S. and Yang, H.T.Y. (1996), "Simple ATMD control methodology for tall building subject to wind loads", *J. Struct. Eng.* ASCE, **122**(1), 83-91.
- Brancaloni, F. (1992), "The construction phase and its aerodynamic issues", *Aerodynamics of Large Bridges* (Larsen A. ed.), A. A. Balkema, Rotterdam, Holland, 17-158.
- Clough, R.W. and Penzien, J. (1993), *Dynamics of Structures*, Second Edition, McGraw-Hill: New York.
- Dung, N.N., Miyata, T., and Yamada, H. (1996), "Structural control in consideration of flutter response in long span bridges", *Proc. the 2nd Int. Workshop on Structural Control*, Hong Kong, 152-162.
- Dung, N.N., Miyata, T., and Yamada, H. (1996), "Application of robust control to the flutter in long span bridges", *J. Struct. Eng. Earthq. Eng.*, JSCE, **42A**, 847-853.
- Fujino, Y. and Sun, L.M. (1993), "Vibration control by multiple tuned liquid dampers (MTLDs)", *J. Struct. Eng.*, ASCE, **119**(12), 3482-3502.
- Fujino, Y., Sun, L., Pacheco, B.M., and Chaiseri, P. (1992), "Tuned liquid damper (TLD) for suppressing horizontal motion of structures", *J. Eng. Mech.*, **118**(10), 2017-2030.
- Gu, M., Chen, S.R., and Chang, C.C. (1999), "Buffeting control of the Yangpu Bridge using multiple tuned mass dampers", *Proc. the 10th Int. Conf. on Wind Engineering*, (Larsen A. et al. ed.), Copenhagen, Denmark, **2**, 893-898.
- Gu, M., Chang, C.C., Wu, W., and Xiang, H.F. (1998), "Increase of critical flutter wind speed of long span bridges using tuned mass damper", *J. Wind Eng. and Ind. Aerod.*, **73**, 111-123.

- Jain, A., Jones, N.P., and Scanlan, R.H. (1998), "Effect of modal damping on bridge aeroelasticity", *J. Wind Eng. Ind. Aerod.*, **77-78**, 421-430.
- Jain, A., Jones, N.P., and Scanlan, R.H. (1996), "Coupled flutter and buffeting analysis of long-span bridges", *J. Struct. Eng.*, ASCE, **122**(7), 716-725.
- Jangid, R.S. and Datta, T.K. (1997), "Performance of multiple tuned mass dampers for torsionally coupled system", *J. Earthq. Eng. Struct. Dyn.*, **26**(3), 307-317.
- Kihara, H., Kunitsu, H., and Asami, Y. (1993), "Structural design and wind resistance of Fukuoka Tower with TMD", *Proc. Struct. Cong. Struct. Eng. in Natural Hazard Mitigation*, ASCE, New York, N.Y., 646-651.
- Kobayashi, H. and Nagaoka, H. (1992), "Active control of flutter of a suspension bridge", *J. Wind Eng. Ind. Aerod.*, **41-44**, 143-151.
- Kobayashi, H., Ogawa, R., and Taniguchi, S. (1998), "Active flutter control of a bridge deck by ailerons", *Proc. the 2nd World Conf. on Structural Control*, (Kobori T. et al. ed.), Kyoto, Japan, **3**, 1841-1848.
- Lin, Y.Y., Cheng, C.M., and Lee, C.H. (2000), "A tuned mass damper for suppressing the coupled flexural and torsional buffeting response of long-span bridges", *J. Engrg. Struct.*, Elsevier, **22**, 1195-1204.
- Miyata, T., Yamada, H., Dung, N.N., and Kozama, K. (1994), "On active control and structural response control of the coupled flutter problem for long span bridges", *Proc. of 1st World Conf. on Structural Control*, Los Angeles, USA, VI, 1, WA4-40-49.
- Nobuto, J., Fujino, Y., and Ito, M. (1988), "A study on the effectiveness of TMD to suppress a coupled flutter of bridge deck", *J. Struct. Mech. Earthq. Eng.*, JSCE, 398/1-10, 413-416 (in Japanese).
- Phongkumsing, S., Wilde, K., and Fujino, Y. (1998), "Analytical study on flutter suppression by eccentric mass method on 3D full suspension bridge model", *Proc. the 2nd World Conf. on Struct. Control*, Kyoto, Japan, **3**, 1797-1806.
- Sakai, F., Takaeda, S., and Tamaki, T. (1991), "Tuned liquid column damper (TLCD) for cable-stayed bridges", *In: Proceeding Specialty Conf. on Innovation in cable-stayed bridges*, Fukuoka, Japan, 197-205.
- Scanlan, R.H. and Tomko, J.J. (1971), "Airfoil and bridge deck flutter derivatives", *J. the Engrg. Mech. Div.*, ASCE, **97**(6), 1717-1737.
- Sun, L.M., Fujino, Y., Pacheco, B.M., and Chaiseri, P. (1991), "Modeling of tuned liquid damper (TLD)", *Proceeding of 8th Int. Conf. on Wind Engineering*, IAWQ, London, Canada.
- Weisne, K.B. (1979), "Tuned mass damper to reduce building wind motion", *ASCE, Convention and Exposition, Preprint 3510*, ASCE, New York, N.Y.
- Wilde, K. and Fujino, Y. (1998), "Aerodynamic control of bridge deck flutter by active surfaces", *J. Eng. Mech.*, ASCE, **124**(7), 718-727.
- Wilde, K., Fujino, Y., and Kawakami, T. (1998), "Analytical and experimental study on passive aerodynamic control of flutter of bridge deck section", *J. Wind Eng. Ind. Aerod.*, **80**(1-2), 105-119.
- Wilde, K., Fujino, Y., and Prabis, V. (1996), "Effects of eccentric mass on flutter of long span bridge", *Proc. 2nd Int. Workshop on Structural Control*, Hong Kong, 564-574.
- Xue, S.D., Ko, J.M. and Xu, Y.L. (2000), "Tuned liquid column damper for suppressing pitching motion of structures", *J. Eng. Struct.*, **23**, 1538-1551.
- Xu, Y.L., Samali, B. and Kwok, K.C.S. (1992), "Control of along-wind response of structures by mass and liquid dampers", *J. Eng. Mech.*, ASCE, **118**(1), 20-39.
- Yoneda, M., Fujino, Y., Kande, H., Yamamoto, A., Miyamoto, Y., Ando, O., Maeda, K., and Katayama, T. (1989), "A practical study of tuned liquid damper with application to the Sakitama Bridge", *J. Wind Eng.* (in Japanese), **41**, 105-106.

## Appendix - A

Matrices  $[\mathbf{A}^F]$  and  $[\mathbf{B}^F]$  can be written as

$$[\mathbf{A}^F] = \left[ \begin{array}{c|c} \begin{matrix} H_1^* L_1 & & & \\ 0 & \text{zeros} & & \\ & H_1^* L_2 & & \\ & 0 & \ddots & \\ & \text{zeros} & & H_1^* L_n \\ & & & 0 \end{matrix} & \begin{matrix} / & BH_2^* L_1 \\ & 0 & \text{zeros} \\ & & BH_2^* L_2 \\ & & 0 & \ddots \\ & \text{zeros} & & BH_2^* L_n \\ & & & 0 \end{matrix} \\ \hline \begin{matrix} BA_1^* L_1 & & & \\ 0 & \text{zeros} & & \\ & BA_1^* L_2 & & \\ & 0 & \ddots & \\ & \text{zeros} & & BA_1^* L_n \\ & & & 0 \end{matrix} & \begin{matrix} / & B^2 A_2^* L_1 \\ & 0 & \text{zeros} \\ & & B^2 A_2^* L_2 \\ & & 0 & \ddots \\ & \text{zeros} & & B^2 A_2^* L_n \\ & & & 0 \end{matrix} \end{array} \right]_{(4n \times 4n)} \quad (A1)$$

and

$$[\mathbf{B}^F] = \left[ \begin{array}{c|c} \begin{matrix} \frac{H_4^*}{B} L_1 & & & \\ 0 & \text{zeros} & & \\ & \frac{H_4^*}{B} L_2 & & \\ & 0 & \ddots & \\ & \text{zeros} & & \frac{H_4^*}{B} L_n \\ & & & 0 \end{matrix} & \begin{matrix} / & H_3^* L_1 \\ & 0 & \text{zeros} \\ & & H_3^* L_2 \\ & & 0 & \ddots \\ & \text{zeros} & & H_3^* L_n \\ & & & 0 \end{matrix} \\ \hline \begin{matrix} A_4^* L_1 & & & \\ 0 & \text{zeros} & & \\ & A_4^* L_2 & & \\ & 0 & \ddots & \\ & \text{zeros} & & A_4^* L_n \\ & & & 0 \end{matrix} & \begin{matrix} / & BA_3^* L_1 \\ & 0 & \text{zeros} \\ & & BA_3^* L_2 \\ & & 0 & \ddots \\ & \text{zeros} & & BA_3^* L_n \\ & & & 0 \end{matrix} \end{array} \right]_{(4n \times 4n)} \quad (A2)$$

The combined bridge-TMD system matrices also can be evaluated as

$$[\mathbf{M}_{BT}] = \begin{bmatrix} \mathbf{M}^V & 0 & / & \text{zeros} \\ 0 & \mathbf{M}_T^V & / & \\ \text{-----} & / & \text{-----} & \\ & / & \mathbf{M}^\theta & 0 \\ \text{zeros} & / & 0 & \mathbf{I}_T^\theta \end{bmatrix}_{(4\mathbf{n}+2)(4\mathbf{n}+2)} \quad (\text{A3})$$

$$[\mathbf{K}_{BT}] = \begin{bmatrix} OR & OR & OR & 0 & / & & & \\ OR & K_{OR}^V + K_T^V & OR & -K_K^V & / & & & \text{zeros} \\ OR & OR & OR & 0 & / & & & \\ 0 & -K_T^V & 0 & K_T^V & / & & & \\ \text{-----} & / & \text{-----} & & & & & \\ & / & OR & OR & OR & 0 & & \\ & / & OR & K_{OR}^\theta + K_T^\theta & OR & -K_T^\theta & & \\ \text{zeros} & / & OR & OR & OR & 0 & & \\ & / & 0 & -K_T^\theta & 0 & K_T^\theta & & \end{bmatrix}_{(4\mathbf{n}+2)(4\mathbf{n}+2)} \quad (\text{A4})$$

and

$$[\mathbf{C}_{BT}] = \begin{bmatrix} OR & OR & OR & 0 & / & & & \\ OR & C_{OR}^V + C_T^V & OR & -C_K^V & / & & & \text{zeros} \\ OR & OR & OR & 0 & / & & & \\ 0 & -C_T^V & 0 & C_T^V & / & & & \\ \text{-----} & / & \text{-----} & & & & & \\ & / & OR & OR & OR & 0 & & \\ & / & OR & C_{OR}^\theta + C_T^\theta & OR & -C_T^\theta & & \\ \text{zeros} & / & OR & OR & OR & 0 & & \\ & / & 0 & -C_T^\theta & 0 & C_T^\theta & & \end{bmatrix}_{(4\mathbf{n}+2)(4\mathbf{n}+2)} \quad (\text{A5})$$

in which  $[\mathbf{M}_{BT}]$ ,  $[\mathbf{K}_{BT}]$  and  $[\mathbf{C}_{BT}]$  are the mass, stiffness and damping matrices of the combined bridge-TMD system. In the matrices *OR* refers to the original bridge component without using TMD.

AK